Yu *et al. Microbial Cell Factories* (2025) 24:51
https://doi.org/10.1186/s12934-025-02681-5

Microbial Cell Factories

RESEARCH Open Access

Enhanced thermostability of nattokinase by rational design of disulfide bond

Kongfang Yu[1†], Liangqi Chen[1,2†], Yaolei Tang[3], Aixia Ma[1,2], Wenhui Zhu[1], Hong Wang[1], Xiyu Tang[1,2], Yuan Li[1,2*] and Jinyao Li[1,2*]

Abstract
Nattokinase, the thrombolytically active substance in the health food natto, nevertheless, its lower thermostability restricts its use in food and pharmaceutical applications. In this study, two heat-resistant variants of nattokinase, designated 50–109 (M1) and 15–271 (M2), were successfully obtained by introducing a disulfide bonding strategy. Their half-lives at 55℃ were found to be 2.50-fold and 5.17-fold higher, respectively, than that of the wild type. Furthermore, the specific enzyme activities of the variants, M1 and M2, were also increased by 2.37 and 1.66-fold, respectively. Meanwhile, the combination of two mutants increased the thermostability of nattokinase by 8.0-fold. Bioinformatics analyses indicated that the enhanced thermostability of the M1 and M2 variants was due to the increased rigidity and structural contraction of the overall structure. Finally, the fermentation process of mutant M1 was optimized to increase the expression of nattokinase. Study provides substantial molecular and theoretical support for the industrial production and application of nattokinase.

Keywords Nattokinase, Disulfide bond, Enzyme synthesis, Thermostability, Bioinformatics design

Introduction

In recent years, the incidence of cardiovascular disease has increased significantly worldwide, and the search for effective and safe thrombolytic drugs has become an important direction in the field of cardiovascular and cerebrovascular disease research [1]. Nattokinase has been widely regarded by the scientific community as a promising drug for the prevention and treatment of cardiovascular and cerebrovascular diseases due to its strong thrombolytic effect and safety since it was discovered in Natto in 1987 [2]. Nevertheless, numerous challenges persist in the industrial production of nattokinase, including poor thermostability and low activity. Among these, the poor thermostability of nattokinase represents a significant hurdle that must be overcome. Currently, nattokinase is predominantly marketed as a health product in the form of enzyme preparations. However, the enzymatic drying and granulation process necessitates a brief period of elevated temperature (170℃), which significantly constrains the industrial production and market application of nattokinase [3].

Many studies have demonstrated that a number of factors influence the thermostability of proteins, including hydrogen bonds and salt bridges, which act in concert to determine the thermostability of protein molecules [4]. Disulfide bonds are formed by the oxidation of two

†Kongfang Yu and Liangqi Chen contributed equally to this work.

*Correspondence:
Yuan Li
liyuanstc@xju.edu.cn
Jinyao Li
ljyxju@xju.edu.cn
[1]Institute of Materia Medica, College of Pharmacy, Xinjiang University, Urumqi 830017, China
[2]Xinjiang Key Laboratory of Biological Resources and Genetic Engineering, College of Life Science and Technology, Xinjiang University, Urumqi 830017, China
[3]The Third People's Hospital of Xinjiang Uygur Autonomous Region, Urumqi 830000, China

cysteine residues and can be divided into intramolecular and intermolecular disulfide bonds according to the position of the cysteine residue [5]. Disulfide bond is one of the most common post-translational modifications in protein structure. As a covalent bond, disulfide bond has a dissociation energy of about 60 kcal/mol, much higher than that of non-covalent bonds such as hydrogen bond, and plays an important role in the correct folding and three-dimensional structure stability of proteins [6]. Yang et al. identified a novel cellulase from the thermophilic fungus *Thielavia arenaria* XZ7, which showed remarkable thermostability at 90℃ and 100℃ [7]. By studying disulfide bond deletion mutants, they found that the C12-C48 disulfide bond is essential for the thermal adaptation and refolding of the enzyme. The optimum temperature and Tm values of variant C12S were reduced by 10–15 and 8.2℃, respectively. Zhu et al. rationally designed the α-amylase of *Steamy Steobacterium lipophila*, introduced disulfide bonds into the flexible region, and constructed a mutant Amys1 with improved thermostability, whose half-life at 90℃ was increased by about 40 fold [8].

Rational design represents an efficient and labour-saving method for molecular modification. It does not necessitate the construction of a vast mutant library, but rather, only a small number of direct mutants are constructed and screened for the desired mutants [9–12]. Rational design is primarily based on a specific comprehension of the structure, function, catalytic mechanism, and catalytic residues of enzyme molecules [13]. Through bioinformatics analysis of amino acid sequence, advanced structure and function of enzyme molecules and targeted design of mutants, the properties of enzyme molecules can be efficiently improved [14].

In order to comprehend the fundamental challenge of inadequate thermostability in nattokinase and its inability to satisfy the requirements of industrial applications, we have constructed disulfide bonds in nattokinase through the utilisation of a rational design method, thereby substantially enhancing its thermostability [15]. Concurrently, molecular dynamics simulations were conducted to elucidate the molecular mechanism underlying the enhanced thermostability of nattokinase. This theoretical underpinnings will facilitate the rational design of thermostability in analogous enzymes.

Materials and methods

Plasmids, strains, and cultivation conditions

The expression vector was a recombinant plasmid pET-28a-AprY (kanamycin-resistant) containing the full nattokinase peptide (rAprY) from *Bacillus mojavensis* LY-06. *Escherichia coli* BL21 (DE3) served as the host for rAprY expression were carried out in Luria-Bertani (LB) medium (5 g/L yeast extract, 10 g/L tryptone, 10 g/L NaCl, pH 7.0). Isopropyl-beta-D thiogalactopyranoside (IPTG) induced recombinant protein expression.

Site-directed mutagenesis and production of nattokinase variants

Sangon Biotech Co., Ltd. (Shanghai, China) synthesized the primers (Table S1) mutagenesis with primers X-up and X-down and TransStart FastPfu Fly PCR SuperMix (TransGen Biotech) created mutations in the AprY gene of plasmid pET-28a-AprY. Following PCR purification with DMT enzyme, the products were transformed into Escherichia coli DH5α competent cells. Kanamycin selection on LB plates yielded colonies for sequencing by Shanghai Sangon Biotech Co.,Ltd. (Shanghai, China) [16].

Bacterial expression and purification of rAprY and its variants

The method of expression and purification of rAprY and its variants was based on the previous work of Li et al. [17]. *Escherichia coli* BL21 (DE3) cells carrying the pET-28a-AprY expression vector and its variants were grown in LB medium containing 50 μg/mL kanamycin at 37℃. Overexpression was induced by adding IPTG to a final concentration of 0.1 mM when the OD_{600} reached 0.7–0.8. Cells were further grown at 16℃ for 20 h and harvested by centrifugation. The bacterial pellet was resuspended by adding lysis buffer (50 mM NaH_2PO_4, 300 mM NaCl, 10 mM imidazole, 5% glycerol, pH 7.4). The harvested cells were lysed by sonication and centrifuged to remove cell debris. The resulting suspension was then centrifuged at 20,000×g for 30 min at 4℃, and the supernatant was used for subsequent purification at 0–4℃. The rAprY and its variants were purified by column chromatography using the Ni-NTA column (Invitrogen, Carlsbad, CA, USA). After purification to homogeneity, the protein concentration was determined using the Bradford protein assay reagent kit (Beyotime, Shanghai, China).

Assay of thrombolytic activity

Enzymatic characterization of rAprY and its variants employed a tetrapeptide substrate method [18]. Purified nattokinase activity was determined by monitoring the release of p-nitroaniline (p-NA) from the chromogenic substrate succinyl-AAPF-pNA (suc-AAPF-pNA). Reactions were conducted in a 96-well plate at 25℃ using 200 μL of phosphate-buffered saline (PBS, 8 mM Na_2HPO_4, 136 mM NaCl, 2 mM KH_2PO_4, 2.6 mM KCl, pH 7.0-7.2) supplemented with an appropriate amount of enzyme. The reaction was initiated by the addition of suc-AAPF-pNA to a final concentration of 0.25 mM. Continuous monitoring of p-NA production at 405 nm for 3 min was achieved using a SpectraMax®ID5 multimode microplate

reader (Molecular Devices, San Jose, CA, USA). One unit of enzymatic activity was defined as the amount of enzyme that catalyzes the production of 1 μmol of p-NA per minute under the specified assay conditions.

The fibrin plate assay, as described by Li et al. [19], was utilized to assess the thrombolytic activity and thermostability of rAprY variants in their crude form. Briefly, A solution of 4 mg/mL fibrinogen (prepared in a water bath at 37℃), 50 U/mL thrombin, and 1% agarose (prepared in a water bath at 60 °C) was prepared using a sodium barbital buffer (comprising 10.1 g/L barbital sodium, 7.4 g/L NaCl, 1 g/L gelatin, and a pH of 7.8). A total of 7.5 mL of the 1% agarose solution was combined with 7.5 mL of the 4 mg/mL fibrinogen solution and 0.4 mL of the 50 U/mL thrombin solution. The resulting mixture was then poured into the plate and left at room temperature for 30 min. A total of 1 μL of the nattokinase crude enzyme was added to the aforementioned plate, and the diameter of the transparent circle (mm^2) was calculated after culturing at 37 °C for 18 h. The fibrinolytic activity was then measured using a urokinase standard as a control.

Biochemical characterization of rAprY and its variants

Optimal temperature and pH were determined using the tetrapeptide substrate method. Purified enzyme solutions were incubated at various temperatures (20–70℃) and pH values (3–11) for optimal activity. Citric acid buffer (pH 3.0–5.0), sodium phosphate buffer (pH 6.0–8.0), and sodium carbonate buffer (pH 9.0–11.0) were used to maintain the desired pH ranges. Thermostability and pH stability were assessed by incubating purified wild-type and mutant enzyme solutions in appropriate buffers for 4 h at various temperatures or pH values. Residual enzyme activity was then measured using the tetrapeptide substrate method, with the highest activity designated as 100%. Half-life ($t_{1/2}$) of the wild-type and mutant enzymes was determined by incubating the purified solutions at 55 °C for varying time points (10–60 min). Untreated enzyme activity served as the 100% reference point. The number of disulfide bonds in WT and mutant rAprY variants was determined using Ellman's method with sulfhydryl detection kits (BestBio, Shanghai, China).

Determination of the kinetic parameters

Kinetic parameters (K_m and K_{cat}) of rAprY and its variants were determined using suc-AAPF-pNA as the substrate. The substrate concentration was varied from 0.05 to 4 mM in phosphate-buffered saline (PBS; 8 mM Na_2HPO_4, 136 mM NaCl, 2 mM KH_2PO_4, 2.6 mM KCl, pH 7.0-7.2) at 25 °C. Michaelis-Menten kinetics were employed to calculate the parameters using GraphPad Prism 8 software (San Diego, CA, USA). Data represent the mean values obtained from three independent experiments.

Bioinformatics analysis

The protein sequences of rAprY and its variants were submitted to the AlphaFold2 workstation, which generated accurate structural models (https://alphafold.ebi.ac.uk, accessed on 19 May 2024) [20]. The protein models were analysed using the PROCHECK module of SAVES 6.0 (https://saves.mbi.ucla.edu/, accessed on 19 May 2024) to generate a Ramachandran plot and assess the model's reliability [21]. The AprY primary sequence conservation was calculated using the Consurf-DB online software (https://consurf.tau.ac.il/consurf_index.php, accessed on 19 May 2024) [22]. Disulfide by design 2.0 software was used to design the disulfide bond of nattokinase (http://cptweb.cpt.wayne.edu/DbD2/, accessed on 19 July 2024) [23] The B-factor of modeled protein amino acid residues was calculated using the Predy Flexy server (https://www.dsimb.inserm.fr/dsimb_tools/predyflexy/index.html, accessed on 19 May 2024) [24].

Molecular dynamics (MD) simulations were performed on the protein models using YASARA software [25]. The initial setup involved hydrogen bond network optimization to improve solute stability [26]. Protonation states of protein residues were adjusted using pKa predictions for a physiological pH of 8.0. NaCl ions were added to a final concentration of 0.9% with an appropriate counterion (Na^+ or Cl^-) to maintain charge neutrality. Steepest descent and simulated annealing minimizations were employed to eliminate steric clashes. The simulations were then run for 100 ns using the AMBER14 force field for the solute and the TIP3P water model. A cutoff of 10 Å was applied for van der Waals interactions [27]. Long-range electrostatics were treated with the particle-mesh Ewald method using a grid spacing of 1.0 nm. Integration of the equations of motion employed an established algorithm [28]. Bonded and non-bonded interactions were computed with a multiple time step scheme of 1.25 fs and 2.5 fs, respectively. The simulations were conducted under NPT ensemble conditions at a temperature of 328.15 K and a pressure of 1 atm. Analysis of the solute root mean square deviation (RMSD) as a function of simulation time indicated an equilibration period of 50 ns, which was excluded from further analysis. Trajectory analysis was performed using various YASARA utilities: macro md_run for simulation execution, md_analyze for calculating radius of gyration (Rg), potential energy, solvent accessible surface area (SASA), protein secondary structure content, and hydrogen bond count, and md_analyzeres for obtaining root mean square fluctuation (RMSF) values. Protein structure visualization was achieved using PyMOL software.

Steered molecular dynamics simulation (SMD), which is used to illustrate how biomolecules respond to external mechanical manipulations at the atomic level, mimics the principles of atomic force microscopy (AFM) [29].

The equations of motion were integrated using a multiple timestep of 1.25 fs for bonded intraactions and 2.5 fs for non-bonded interactions at a temperature of 298K and a pressure of 1 atm (NPT ensemble) using algorithms previously described in detai. After a 3 ps equilibration period, a minimum acceleration of 2000 pm/ps²was applied to all ligand atoms, along with non-bonded forces every 2.5 fs. The ligand has a mass of 624.24 Daltons, and using the equation F = m×a, this results in a pulling force of [2000 × 624.24 × 0.00166] picoNewtons. The pulling direction was determined as the vector connecting the centers of mass of the receptor and ligand, and was continuously updated to account for rotations of the complex [30]. The simulation continuously updated the maximum distance between the centers of mass of the receptor and ligand. If the distance did not increase for 400 simulation steps, the acceleration was increased by 500 pm/ps^2. When the maximum distance grew with a 'MaxDisSpeed' faster than 4000 m/s, the acceleration was scaled down by a factor of 1-(1-4000/MaxDisSpeed)^2, but not below the initial minimum. This check occurred every 20 simulation steps. The simulation ended when the ligand had moved 15 Å away. The peak pulling force and total work done were calculated to correlate with the binding strength.

Optimization of the fermentation process of 50–109 (M1) variant production

The bacterial strains *Escherichia coli* BL21(DE3), *Escherichia coli* Shuffle T7, *Escherichia coli* Rosetta gamiB(DE3), *Escherichia coli* Rosetta(DE3) and *Escherichia coli* OrigamiB(DE3) were employed as hosts for the heterologous expression of the M1 variant proteins. The induced bacterial solution was subjected to sonication, and the resulting supernatant was analysed by SDS-PAGE. The grey value of the total and target protein bands produced by SDS-PAGE was determined using Fiji ImageJ software. In order to investigate the effect of different single-factor conditions on nattokinase production, the enzyme activity of M1 crude enzyme, measured by the fibrin plate method, was employed as an examination index for single-factor optimisation experiments. The optimal results of each round of optimisation were accumulated and incorporated into the subsequent round of optimisation. LB medium was used for the optimisation of enzyme production conditions, and the factors examined included fermentation time (14 h, 16 h, 18 h, 20 h, 22 h), fermentation temperature (14℃, 16℃, 18℃, 20℃, 22℃), bottling volume (10%, 20%, 30%, 40%, 50%), initial pH (5, 6, 7, 8, 9), and inoculum volume (0.5%, 1.0%, 1.5%, 2.0%, 2.5%). The optimal fermentation broth conditions for the production of M1 variants were determined by orthogonal experiments on the factors that had a greater influence on rAprY.

Results and discussion

Rational design of disulfide bonds

Disulfide bonds are covalent bonds that link different peptide chains or two cysteine residues in the same peptide chain and play a role in stabilising the steric conformation in protein molecules [31]. In this study, the disulfide bond of nattokinase was designed using design 2.0 (DbD2) software, and a total of 49 mutant pairs were obtained (Table 1). On this basis, the number of candidate mutation sites was compressed to 41 by removing the mutation sites close to the catalytic active site (6 Å). The β-carbon atoms of the two cysteines that make up the protein disulfide bond are generally within 4 Å of each other and the spacer sequences are generally greater than 25 amino acid residues, so we used the rules described above to screen candidate mutants and shorten the number of mutants to 8 pairs (S49C-K94C, N123C-A228C, A230C-V270C, A15C-Q271C, F50C-N109C, K12C-Q271C, T22C-S87C and A85C-A232C). Considering that the highly conserved amino acid residues in the protein may have an impact on the catalytic performance of AprY, the highly conserved candidate mutation sites were removed and the number of mutants was reduced to 5 pairs (A230C-V270C, A15C-Q271C, F50C-N109C, K12C-Q271C and T22C-S87C). Regions prone to disulfide bond formation tend to have relatively high mobility, i.e. high b-factor and RMSF values [32]. The B-factor usually reflects the static flexibility of the protein; a higher B-factor value indicates a more flexible or unstable structure. As the static flexibility is closely related to the crystal quality and structural resolution of the protein, the B-factor value will differ even for different crystal structures of the same protein [33]. Therefore, further analysis of the dynamic flexibility of nattokinase enzymes is needed to further identify candidate mutants capable of forming disulfide bonds. We performed molecular dynamics simulations at 328.15 K for 100 ns using the wild-type AprY obtained from homology modelling. The flexible region of AprY was screened by analysing the RMSF values and four mutants, F50C-N109C and A15C-Q271C were finally identified (Table 1 and Figure S1). Therefore, two mutants, 50–109 (M1) and 15–271 (M2), were selected for the next study.

Purification and characterization of 50–109 (M1), 15–271 (M2) and 50–109/15–271 (SS) variants

Variants M1 and M2 were constructed by site-specific mutation. SDS-PAGE analysis showed that the mutant was successfully expressed in Escherichia coli BL21(DE3) (Figure S2). The disulfide bond detection kit was used to verify the formation of disulfide bonds introduced in the mutants [34]. It can be seen that free thiols were not detected in both M1 and M2 variants without TCEP treatment, indicating that both cysteines formed disulfide

Table 1 Screening results of candidate sites

Candidate site	Distance from catalytic centre (Å)	Distance of β-carbon atoms between candidate sites (Å)	Conservation*	averageB-factor (Å)	averageRMSF (Å)
T255C-L267C	15.5	4.3	3	18.2	5.97
A153C-S191C	8.0	4.2	8	16.92	5.92
L257C-Y263C	15.9	4.2	1	18.43	5.69
R249C-A273C	21.7	4.2	4	18.76	5.68
A254C-G266C	16.9	4.4	8	19.72	5.58
G154Y-G166C	7.5	5.5	9	20.9	5.51
N155C-F189C	8.5	5.1	9	20.08	5.46
D41C-P210C	16.9	11.8	7	21.24	5.39
P57C-K94C	15.6	4.2	3	15.26	5.33
D41C-G80C	18.0	5.0	7	16.83	4.81
D32C-G65C	9.9	3.7	9	13.18	4.79
A169C-A176C	10.7	3.8	7	18.32	4.58
N76C-P86C	18.9	4.2	5	17.8	4.51
V95C-G110C	15.1	5.2	6	15.78	4.42
I205C-M222C	3.8	3.9	7	14.53	4.35
S49C-P57C	19.0	4.1	7	17.02	4.27
E156C-T164C	12.1	3.8	3	19.51	4.27
A179C-A223C	5.6	4.2	7	14.95	4.22
G47C-P57C	9.3	5.0	5	17.84	4.14
A73C-A88C	19.0	4.2	7	15.1	4.11
A200C-A223C	5.6	4.9	9	14.15	4.11
V26C-A232C	17.5	4.2	7	14.92	4.02
L257C-G266C	16.9	4.4	1	18.49	3.98
G70C-A74C	16.3	3.9	7	12.55	3.77
S49C-K94C	15.6	3.9	7	16.18	3.74
S33C-S62C	12.1	3.5	7	17.42	3.55
H39C-L42C	18.8	4.0	8	14.67	3.5
V143C-S173C	17.9	4.1	1	21.08	3.4
A151C-T174C	8.0	4.3	6	17.37	3.19
A254C-K265C	18.3	3.8	8	20.91	2.96
G32C-D60C	10.3	8.1	9	18.36	2.63
N123C-A228C	9.4	3.8	9	12.02	2.51
A230C-V270C	15.0	4.0	5	12.54	2.5
A114C-M119C	19.2	4.2	4	17.21	4.25
W241C-Q245C	23.8	4.0	5	19.22	2.45
S33C-G65C	9.9	4.8	7	14.8	2.34
S37C-V44C	19.9	3.9	1	16.55	2.31
N181C-V203C	10.1	4.0	5	18.14	2.31
A85C-A88C	8.5	3.9	9	14.25	2.29
G34C-K94C	5.9	4.1	9	15.03	2.25
A15C-Q271C	17.2	3.8	1	19.93	2.23
V165C-G193C	12.5	5.3	3	18.41	2.22
S37C-Y58C	19.7	3.9	1	18.39	2.21
F50C-N109C	17.3	4.0	2	16.48	2.16
S24C-S87C	21.4	4.2	4	17.12	1.74
A151C-A169C	8.0	4.0	6	18.56	1.19
K12C-Q271C	19.4	3.8	5	16.91	0.61
T22C-S87C	21.4	3.8	5	17.23	0.59
A85C-A232C	17.2	3.9	9	15.09	2.73

*Candidate amino acid residues were assigned a score of 1 to 9 in descending order of conservation

bonds. After TCEP treatment, one molecule of M1 and M2 variants contained approximately one thiols (Thiol/protein (mol/mol): M1, 1.96 ± 0.22; M2, 1.98 ± 0.19), however, no disulfide bond was observed in wild-type AprY. In order to verify the disulfide bond formation of the individual variants, 100 ns MD was performed at 298.15 K for M1 and M2, respectively, and the last 20 ns were analysed. The results demonstrated that the distance between amino acid residues 50 to 109 of the M1 variant exhibited greater stability compared to the wild type, with a distance less than 4 Å, which met the standard for disulfide bond formation. Conversely, the distance between the M2 variant and the wild type was less pronounced than that observed between the M1 variant and the wild type. However, the average distance of the M2 variant (4.01 Å) was smaller than that of the wild type (4.24 Å), which also met the criteria for disulfide bond formation (Figure S3). The optimum pH, pH stability and optimum temperature of all variants were not significantly altered (Fig. 1A-C). To assess the stability of the variants under high temperature conditions, residual enzyme activity of the pure enzyme of each variant was quantified following incubation at 55℃ for varying periods. Notably, following incubation at 55℃ for one hour, the M2 variant and SS variant exhibited residual fibrinolytic activity in excess of 60%, whereas the wild-type rAprY exhibited residual activity below 20% (Fig. 1D). To characterise the changes in the catalytic properties of each variant, the kinetic parameters of wild-type rAprY and mutants were determined at 25℃ using tetrapeptide substrates as substrates, and all data were fitted by nonlinear regression equations (Table 2). Taking the pure

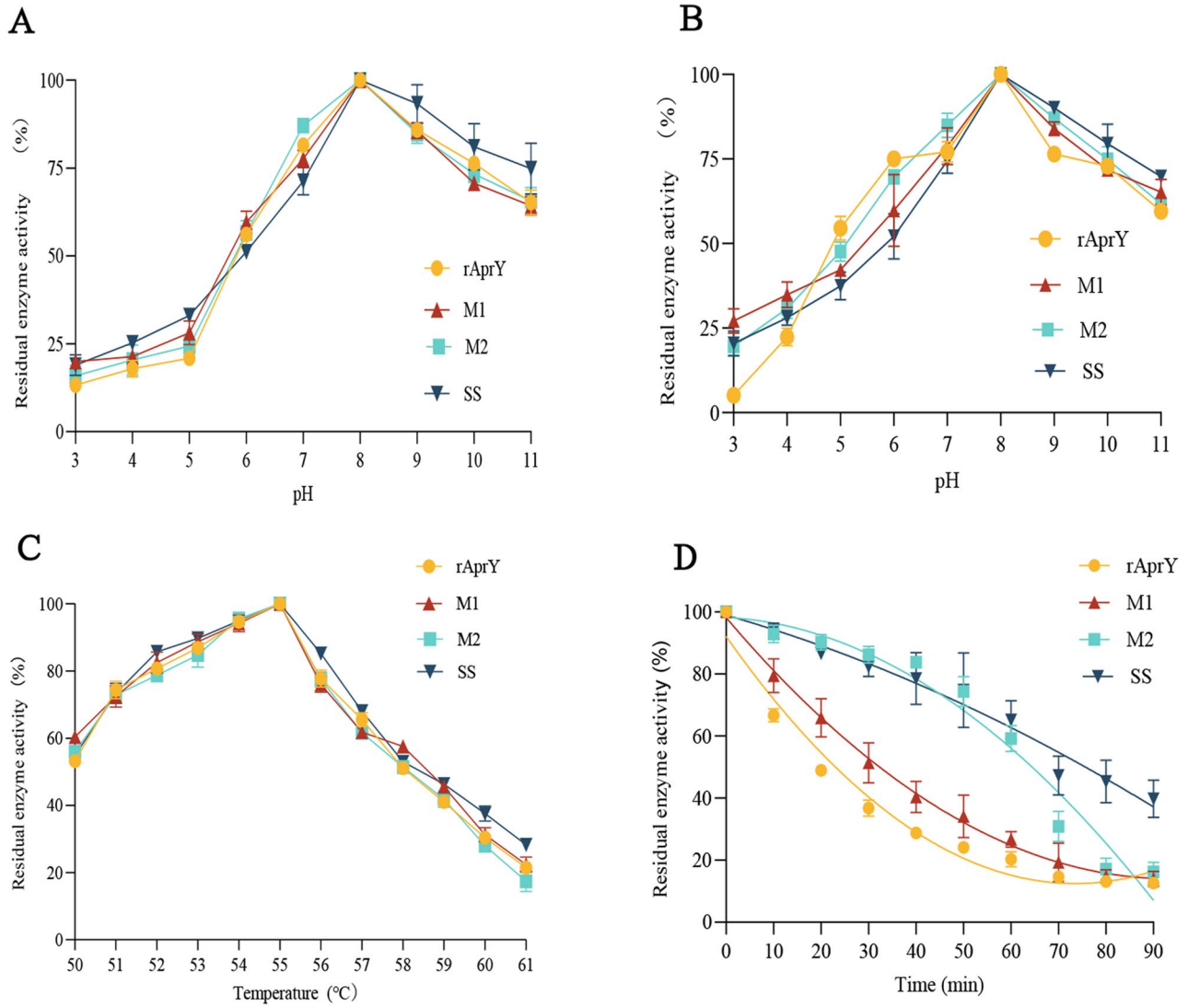

Fig. 1 Enzymatic properties of rAprY and its variants with single-point mutations. (**A**) Optimum pH; (**B**) pH stability; (**C**) Optimum temperature; (**D**) Half-life period

Table 2 Comparison of the enzymatic properties of the wild-type and the single point mutants

	M1	M2	SS	WT
K_m (μmol/L)	1.24 ± 0.03	0.61 ± 0.01	0.59 ± 0.02	1.52 ± 0.11
k_{cat} (S^{-1})	2.29 ± 0.20	1.14 ± 0.22	1.11 ± 0.03	3.75 ± 0.34
K_d (k_{cat}/K_m)	1.65	1.87	1.88	2.5
Specific activity (U/mg)	868.68	608.35	598.52	367.17
half-life (min)	28.7 ± 0.73	59.5 ± 0.32	82 ± 0.57	11.5 ± 0.35
Optimal pH	8	8	8	8
Optimum temperature	55℃	55℃	55℃	55℃

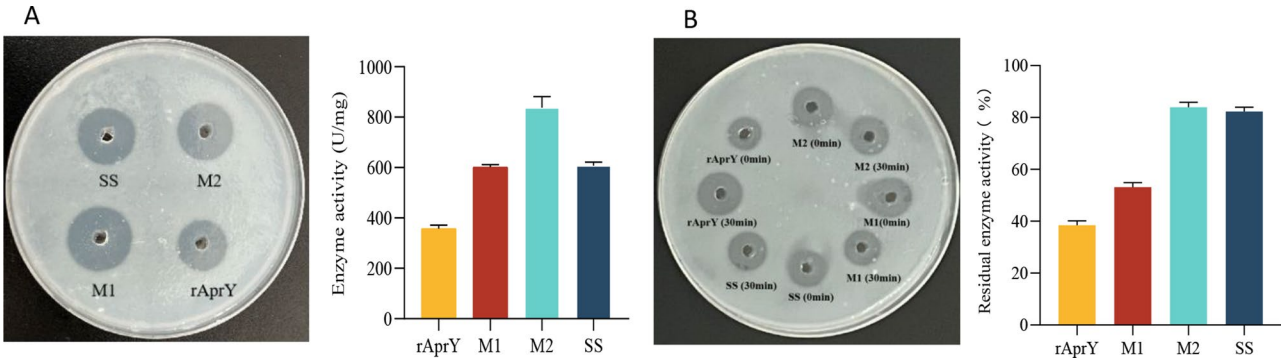

Fig. 2 Nattokinase activity (**A**) and thermostability (**B**) measured using the fibrin plate assay.Samples marked with the plus sign on fibrin plates were those that had been heat-treated (55℃ for 30 min)

enzyme solution and incubating it at 55℃ for 10 min to measure its thermostability, we found that the thermostability of M1, M2 and SS was greatly improved compared with that of the wild type, by 136.6%, 65.7% and 63.0%, respectively; at the same time, the half-lives of M1, M2 and SS were 28.7 min, 59.5 min and 82.0 min, which were 2.5, 5.2 and 7.1 times higher than those of the wild type. Enzymes frequently exhibit a trade-off between stability and activity, indicating that enhancing one property often comes at the expense of the other [35]. In this study, the specific enzyme activities of the three variants M1, M2 and SS were increased by 136.59%, 71.13% and 63.01%, respectively, compared with wild-type rAprY, although their K_d did not change significantly. Accordingly, all mutants had lower K_m values than the WT. It is well known that the Km value indicates the affinity of the substrate for the enzyme, so the increase in specific enzyme activity of all mutants may be due to their improved ability to bind to the substrate. Interestingly, the tetrapeptide substrate assay, which is a common method for the determination of basic serine proteases, sometimes shows that the K_d and k_{cat} value is not fully proportional to the specific enzyme activity, which may be related to the assay method.The above results suggest that the variants obtained in this study were able to overcome the trade-off between the fibrinolytic activity and stability of nattokinase, improving the catalytic activity of nattokinase while improving its thermostability.

The fibrin plate method is affected by incubation time, plate thickness and temperature, and therefore the measured data do not accurately reflect nattokinase activity. However, compared with the tetrapeptide substrate method, the fibrin plate method can more accurately mimic the molecular structure of the thrombus, and is therefore more suitable for the determination of thrombolytic activity in vitro [36]. In order to assess the effect of the introduction of disulfide bonds on nattokinase and to further understand the practical application scenarios of the advantageous mutants with enhanced thermostability in industrial production, we further examined the activity and thermostability of nattokinase and its variants based on the tetrapeptide substrate assay by fibrin plate assay. Initially, the activities of the wild-type rAprY and its variants were calculated by determining the diameter of the transparent circle using the urokinase standard as a standard curve. The enzymatic activities of wild-type rAprY, M1, M2 and SS were 107.9 U/mL,164.4 U/mL, 228.4 U/mL and 163.9 U/mL, respectively, while after incubation for 30 min at 55℃, The residual enzyme activities of wild type rAprY, M1, M2 and SS were 39.6%, 82.6%, 54.3% and 81.1% of those without incubation, respectively (Fig. 2). The results were basically consistent with those measured by tetrapeptide substrate assay. Previous studies have demonstrated that there is an activity-stability trade-off phenomenon for enzymes. This phenomenon can be observed during enzyme engineering modifications, whereby the enhancement of enzyme activity is often accompanied by a decrease in stability [37]. Our study overcame this drawback, and therefore, it

is important to investigate the mechanism of activity and thermostability enhancement of individual variants.

Understanding the mechanism for enhanced catalytic performance of M1 and M2 variants

AlphaFold2 is an AI system created by DeepMind capable of predicting the three-dimensional (3D) structures of proteins based on their amino acid sequences with atomic-level precision [38]. The results of previous experiments showed that M1 and M2 variants have enhanced thermostability compared to wild-type rAprY. In order to deeply investigate the reason for the enhanced thermostability of each variant, this study used the AlphaFold2 online workstation to predict the structure of their proteins by submitting the amino acid sequences of each variant in the workstation, and the accuracy of the protein models was verified by using the PROCHECK module in SAVES 6.0 (PROCHECK generates Ramachandran plots indicating the conformations in which the amino acid residues could theoretically occur) (Figure S4). We selected protein structures with more than 90% of the permissive regions in the Ramachandran plots to perform molecular dynamics simulations (MD) over a period of 100 ns at 328.15 K. In molecular dynamics simulation analysis, the thermostability of proteins is commonly characterised by root-mean-square deviation (RMSD), root-mean-square fluctuation (RMSF), solvent-accessible surface area (SASA) and radius of gyration (Rg). RMSD is an important indicator of molecular dynamics (MD) and represents the smallest arithmetic square root of the position of the backbone atoms throughout the entire motion with respect to the position of the initial structural backbone atoms [39]. It is an indicator of whether or not the simulated system is in equilibrium.When the RMSD value remains stable at a certain stage during the simulation, it indicates that the simulated system has reached basic dynamic equilibrium and the data derived from the simulation are reliable. At the same time, RMSD is also an important factor to characterise the molecular rigidity [40]. The results of the MD indicate that the values stabilise at 1.3–1.5 Å after 50 ns, indicating that the potential and the total energy of the system have reached a stable state (Fig. 3A). This allows for further analysis of the other indexes. In order to facilitate subsequent comparison, all MD data were analysed using data from 50 ns onwards.

After averaging the RMSD values for the last 50 ns of the M1 and M2 variant we found that compared to the wild type, the M1 and M2 variants RMSD decreased significantly (29.81% and 11.9% compared to the wild type rAprY, respectively), indicating a significant increase in the rigidity of the mutant; Correspondingly, Rg, SASA values and the number of solute-solvent hydrogen bonds were reduced in variants M1 and M2, suggesting that the overall tighter structure of variants M1 and M2 is an important factor in their improved thermostability

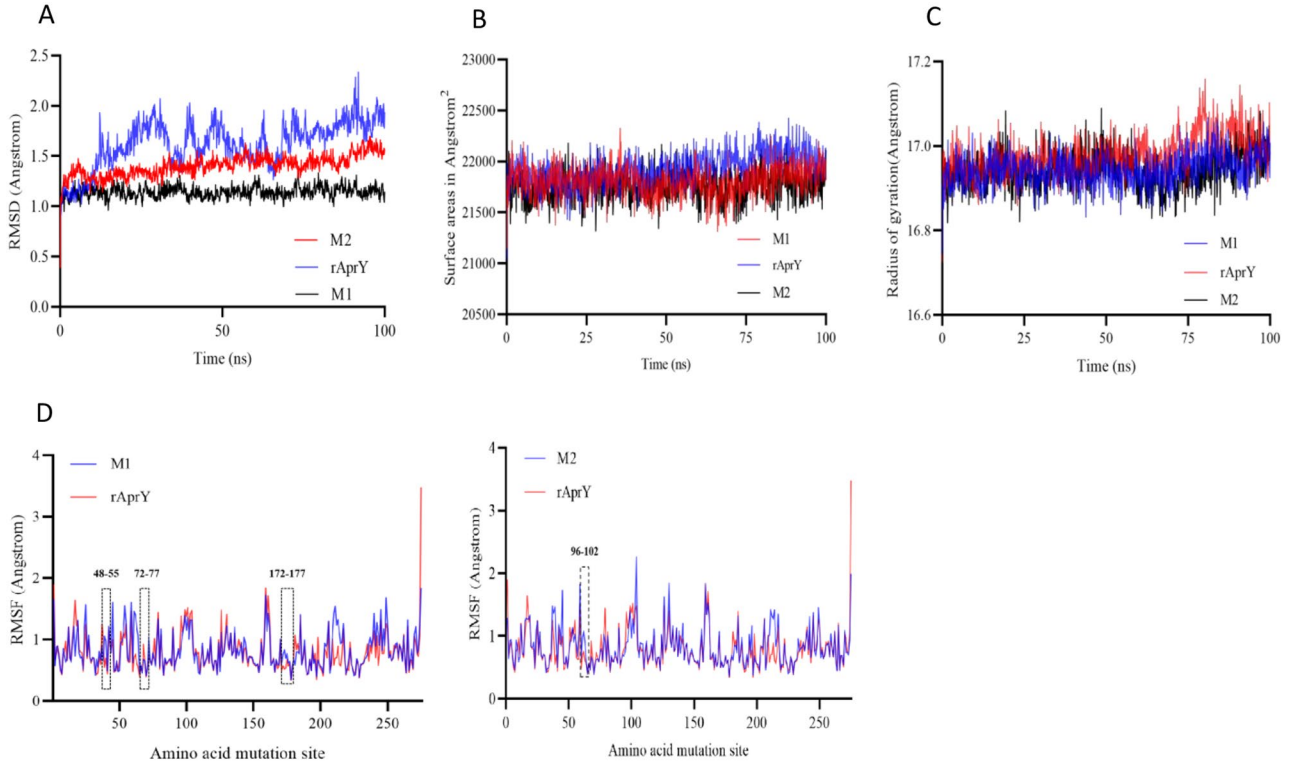

Fig. 3 MD simulation results of AprY and its variants at 328.15 K for 100ns: (**A**) RMSD; (**B**) SASA; (**C**) Rg; (**D**) RMSF

(Fig. 3B-C and Table S2). Secondary structure calculations for variants M1 and M2 showed that although the secondary structure composition of each variant was essentially unchanged compared to wild-type rAprY, their dihedral angle potential energy changed significantly compared to wild-type rAprY (Table S2). The results indicated that although the tertiary structure of the each variant remained largely unaltered, the change in dihedral angle potential energy suggested that the internal interactions of the M1 and M2 variants protein had undergone a transformation, which might be a crucial factor in the enhancement of thermostability of the M1 and M2 variants.

The stability of proteins not only depends on the overall structure, but the increase of local structural rigidity also plays an important role in maintaining the stability of protein structure [41]. The RMSF value represents the fluctuation amplitude of a single amino acid residue from its original position at a specific equilibrium time point within the simulation system. Consequently, RMSF can be employed to reflect the change in local amino acid stability. It is generally accepted that a lower RMSF value indicates a reduction in flexibility and an increase in thermostability in this region [42]. The RMSF of the region encompassing the two mutation sites (amino acid residues 109 and 48–55) in varirant M1 exhibited a slight decline, suggesting that the rigidity of the local structure of the mutation site augmented following the mutation (Fig. 3D). This may be one of the contributing factors to the enhanced thermostability. For the M1 variant, it is noteworthy that a notable reduction in RMSF was observed in the region encompassing amino acid residues 72 to 77, 170 to 174, which is situated within the Ca^{2+} binding site region of nattokinase (Fig. 3D). The Ca^{2+} binding site of nattokinase has been demonstrated to be associated with its thermostability. Consequently, we postulated that the augmented rigidity of the Ca^{2+} binding site region may facilitate Ca^{2+} binding to the protein, which in turn enhances stability [43]. The amino acid residues 208–218 located in the outer region of the catalytic pocket of rAprY, and the increased rigidity of variants M1 in this region can ensure that the nattokinase binding pocket retains its normal conformation at high temperature (Fig. 3D). In contrast to the M1 variant, the M2 variant exhibited a reduction in RMSF in the 96–102 loop region, with the exception of the 174 amino acid residue (Fig. 3D). It has been reported that nattokinase variants S78T and Y217K, which exhibit increased stability, have reduced RMSF around position 100 [44]; In contrast, the nattokinase M4 mutant, which also exhibits increased stability and activity, has increased RMSF at positions 95–105 under high temperature. These results indicate that the 96–102 loop region of nattokinase plays an important role in the catalytic activity of nattokinase.

To explain the mechanism underlying the enhanced fibrinolytic activity of the nattokinase M1 and M2 variants compared with the wild type, MD of variant and wild-type rAprY at 298.15 K for 100 ns were investigated. Although the RMSF of M1 was largely unchanged compared to the wild-type M2 variant, a significant change in the secondary structure composition of the Ser221 region (active centre) was observed in both variants 50 ns (50 to 100 ns) after MD reached stabilisation. This observation is indicative of the more stable secondary structure exhibited by M1 and M2 (Fig. 4A, Figure S5). Correspondingly, the volume and specific surface area of the M1 and M2 mutant active centres increased accordingly, and the docking result showed that the distances of Ser221 residues from wild-type rAprY, M1 and M2 to the substrate peptide bond carbonyl carbon are 4.8 Å, 3.8 Å and 3.4 Å, respectively (Table S3 and Figure S6). In conclusion, it can be hypothesised that the M1 and M2 mutations may indirectly impact the active centre conformation, which in turn exerts an influence on their catalytic activity. Steered dynamics simulation verified the above conjecture: The analysis of Steered kinetic simulations of the tetrapeptide substrates with nattokinase revealed that the ligand binds more tightly to the active centre sites of variants M1 and M2 than to the wild-type rApr. This is evidenced by a more stable hydrophobic interaction of amino acid residue 221 with the substrate compared to the wild-type rAprY, suggesting that the active site of variant M1 and M2 better interacts with the tetrapeptide substrate and thus improves enzymatic efficiency (Fig. 4B). The MD results of each mutant after docking with the substrate also corroborate the aforementioned conclusion, as evidenced by a 30% increase in the number of hydrogen bonds formed by the interaction of the ligand with the surrounding receptor in mutants M1 and M2 relative to the wild-type rAprY, and a considerable rise in the number of hydrogen bonds formed by the interaction of each atom in the ligand of the mutant complexes with the surrounding receptor.

Fermentation process optimisation to enhance the yield of M1 variant

The utilisation of Escherichia coli engineering strains for the expression of heterologous proteins with diverse functions offers several advantages, including a transparent genetic background, straightforward technical manipulation, simple culture conditions, and the potential for large-scale cultivation [45]. Accordingly, a comparison was conducted to assess the impact of five *Escherichia coli* engineering strains, namely *Escherichia coli* BL21 (DE3), *Escherichia coli* SHuffle T7, *Escherichia coli* Rosetta gamiB (DE3), *Escherichia coli* Rosetta (DE3), and *Escherichia coli* OrigamiB (DE3), on the expression of mutant M1. In the absence of any substantial

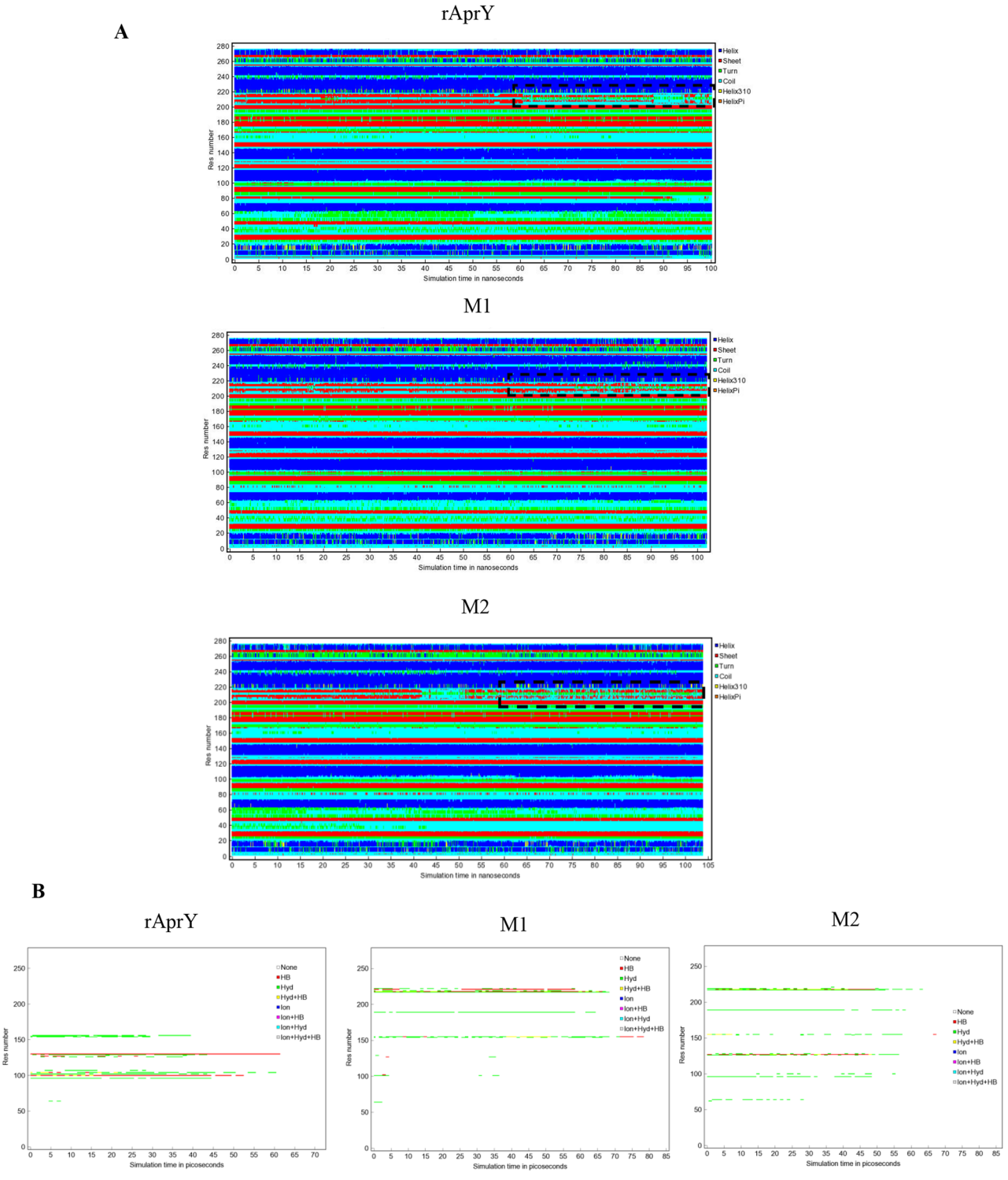

Fig. 4 (**A**) Changes in the secondary structure corresponding to each amino acid residue during MD at 298.15 K; (**B**) Changes in substrate interaction with wild-type rAprY, M1 and M2 variants during steered dynamics simulations

alterations in cell concentration, the recombinant variant M1 exhibited the most pronounced intensity ratio of target bands and the highest activity of crude enzyme. This finding suggests that the Escherichia coli SHuffle T7 strain is particularly conducive to the heterologous expression of the combined variant M1 (Fig. 5A and Figure S7). This may be attributed to the fact that the expression of the genome-integrated DsbC gene of the

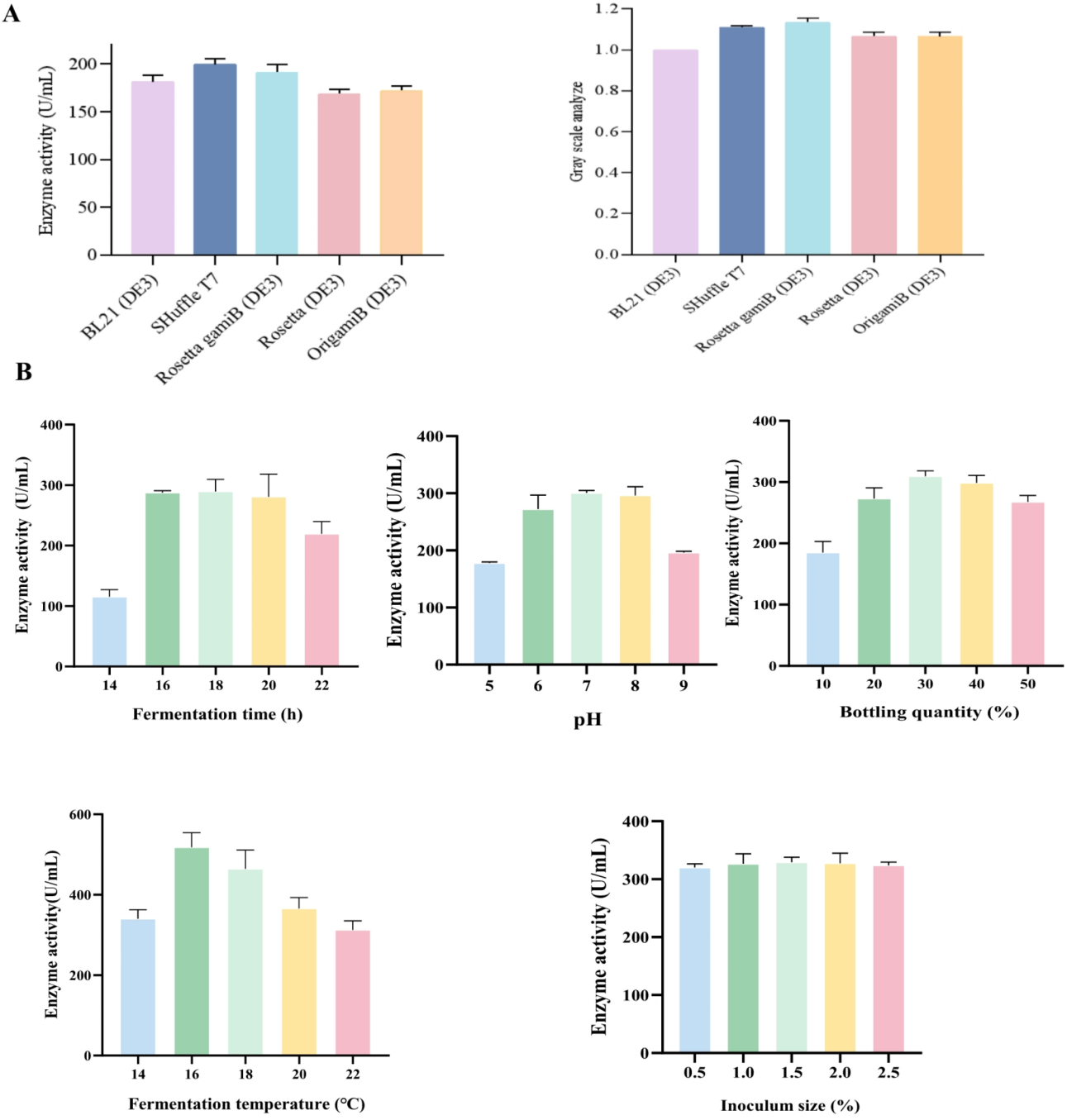

Fig. 5 (**A**) Enzyme activity and Gray-scale scanning analysis of supernatants from different hosts; (**B**) Effects of different induction time, pH, bottling volume, induction temperature and inoculum volume on the production of nattokinase

Escherichia coli SHuffle T7 strain facilitates the correct folding of the protein [46].

The heterologous expression of nattokinase in *Escherichia coli* is characterised by low expression levels and susceptibility to inclusion body formation [47]. Consequently, we conducted a sequential optimisation of the fermentation conditions (induction time, pH, bottling volume, induction temperature, inoculum volume) of the M1 variant in *Escherichia coli* SHuffle T7. The induction time was identified as a key determinant of soluble protein expression [48]. Our single factor experiment, which varied the induction time, demonstrated that 18 h represented the optimal induction time for the M1 variant, with an expression level of 289.27 U/mL. The pH of the fermentation broth had a significant impact on the metabolism and enzyme expression in *Escherichia coli*

Table 3 Experimental results and analysis of L9 (34) orthogonal experiments for nattokinase production

Test Number	Factor				Enzyme activity (U/mL)
	A	B	C	D	
1	1	1	1	1	297.7
2	2	2	2	1	317.1
3	3	3	3	1	327.2
4	4	3	1	2	325.5
5	5	1	2	2	326.9
6	6	2	3	2	356.3
7	7	2	1	3	297.1
8	8	3	2	3	311.2
9	9	1	3	3	341.6
K1	K1	306.767	321.77	322.07	
K2	K2	318.43	328.07	323.50	
K3	K3	341.70	317.07	321.33	
R	R	34.93	11.00	2.17	

[49]. The M1 variant expression was further elevated to 453.34 U/mL when the pH was 7. A single factor experiment was conducted to determine the optimal volume of bacterial solution to be bottled. The results indicated that a volume of 30% of the total bottling volume resulted in optimal expression, with a value of 309.54 U/mL. In light of these findings, further investigation was conducted to examine the influence of induction temperature and inoculum volume on the expression of the M1 variant. The expression of the M1 variant at a concentration of 311.26 U/mL and 327.55 U/mL was achieved simultaneously under the conditions of an induction temperature of 20 °C and a 2% inoculum quantity.

In light of the aforementioned outcomes, the following variables were selected for the orthogonal array experiment: bottling volume, pH, induction temperature and induction time (Table S4). The statistical analysis of the fermentation data was conducted using Minitab 16. The results indicated that pH was the most significant factor, followed by bottling volume, induction temperature and induction time (Table 3). The optimal concentrations of bottling volume, pH, induction temperature and induction time for high-level nattokinase production were determined to be 20%, 7, 20 °C and 18 h, respectively. Under this fermentation condition, the optimal enzyme yield was 356.3 U/mL, which was 2.16 times higher than that before optimization.

Conlusion

In this study, an effective strategy to improve the catalytic performance of nattokinase was explored. For the M1 mutant with improved enzyme activity and thermal stability, the host strain with the highest protein production was selected, and single factor optimization and orthogonal experiments were performed to obtain the optimal fermentation conditions. These results have important guiding significance for the large-scale production of nattokinase, and have potential industrial production and application value. This provides a new oral dosage form for the use of nattokinase, and its combination with other drugs may provide a new oral dosage form for the treatment of thrombophilia or cardiovascular diseases.

Supplementary Information

The online version contains supplementary material available at https://doi.org/10.1186/s12934-025-02681-5.

Supplementary Material 1

Author contributions

Y.L. and J.L.: conceptualization; Y.L. and K.Y.: methodology; Y.T, H.W. and L.C.: software; Y.L., L.C. and W.Z.: validation; L.C., X.T., and A.M.: formal analysis, investigation, data curation, and visualization; Y.L. and J.L.: resources; Y.L., K.Y. and L.C.: writing—original draft preparation; Y.L and L.C.: writing—review and editing; J.L. and Y.L.: supervision; Y.L.: project administration and funding acquisition. All authors have read and agreed to the published version of the manuscript.

Funding

This research was funded by the Science and Technology Department of Xinjiang Uygur Autonomous Region, grant number 2022D01C96,Tianchi Doctoral Program of Xinjiang Uygur Autonomous Region, grant number TCBS202124,and Tianshan Talent Training Program, grant number 2023TSYCLJ0043.

Data availability

No datasets were generated or analysed during the current study.

Declarations

Competing interests

The authors declare no competing interests.

Received: 29 October 2024 / Accepted: 20 February 2025
Published online: 04 March 2025

References

1. Liu C, Du L, Wang S, et al. Differences in the prevention and control of cardiovascular and cerebrovascular diseases [J]. Pharmacol Res. 2021;170:105737.
2. Sumi H, hamada H, Tsushima H, et al. A novel fibrinolytic enzyme (nattokinase) in the vegetable cheese Natto; a typical and popular soybean food in the Japanese diet [J]. Experientia. 1987;43(10):1110–1.
3. Yuan L, Liangqi C, Xiyu T, Jinyao L. Biotechnology, bioengineering and applications of Bacillus nattokinase [J]. Biomolecules. 2022;12(7).
4. Sadeghi M, Naderi-Manesh H, Zarrabi M, Ranjbar B. Effective factors in thermostability of thermophilic proteins [J]. Biophys Chem. 2006;119(3):256–70.
5. Carroll L, Jiang S, Engholm-Keller K, et al. OP-32 - Oxidation of disulfide bonds: a novel pathway to protein glutathionylation [J]. Free Radic Biol Med. 2018;120:S39.
6. Haworth NL, Gready JE, George RA, Wouters MA. Evaluating the stability of disulfide bridges in proteins: a torsional potential energy surface for diethyl disulfide [J]. Mol Simul. 2007;33(6–8):475– 85.
7. Yang H, Zhang Y, LI X, et al. Impact of disulfide bonds on the folding and refolding capability of a novel thermostable GH45 cellulase [J]. Appl Microbiol Biotechnol. 2018;102(21):9183–92.
8. Zhu M, Zhai W, Song R, et al. Enhanced thermostability of Geobacillus stearothermophilus α-Amylase by rational design of disulfide bond and application in corn starch liquefaction and bread quality improvement [J]. J Agric Food Chem. 2023;71(48):18928–42.

9. Brown SD, Babbitt PC. New insights about enzyme evolution from large scale studies of sequence and structure relationships [J]. J Biol Chem. 2014;289(44):30221–8.
10. Chen R. Enzyme engineering: rational redesign versus directed evolution [J]. Trends Biotechnol. 2001;19(1):13–4.
11. Otten R, Liu L, Kenner LR, et al. Rescue of conformational dynamics in enzyme catalysis by directed evolution [J]. Nat Commun. 2018;9(1):1314.
12. ting Sanchez MI. Directed evolution improves the catalytic efficiency of TEV protease [J]. Nat Methods. 2020;17(2):167–74.
13. Rahban M, Zolghadri S, Salehi N, et al. Thermal stability enhancement: fundamental concepts of protein engineering strategies to manipulate the flexible structure [J]. Int J Biol Macromol. 2022;214:642–54.
14. Teufl M, Zajc CU, Traxlmayr MW. Engineering strategies to overcome the Stability-Function Trade-Off in proteins [J]. ACS Synth Biol. 2022;11(3):1030–9.
15. Guo X, jiang L, An Y, et al. Construction and characterization of a myceliophthora thermophila lytic polysaccharide monooxygenase mutant S174C/A93C with improved thermostability [J]. Enzyme Microb Technol. 2023;168:110255.
16. Li Y, Zhu W, Chen L et al. Modification of the active centre of nattokinase to enhance its thermostability using a strategy based on molecular dynamics simulation, steered dynamics simulation, and Conservative prediction [J]. Front Nutr. 2024;11.
17. Li Y, Tang X, Chen L et al. Characterization of a nattokinase from the newly isolated bile Salt-Resistant Bacillus mojavensis LY-06 [J]. Foods. 2022;11(16).
18. Liang X, Zhang L, Zhong J, Huan L. Secretory expression of a heterologous nattokinase in Lactococcus lactis [J]. Appl Microbiol Biotechnol. 2007;75(1):95–101.
19. Li Y, Chen L, Tang X et al. Combined Computer-Aided predictors to improve the thermostability of nattokinase. [J] Foods. 2023;12(16).
20. Skolnick J, Gao M, Zhou H. AlphaFold 2: why it works and its implications for Understanding the relationships of protein sequence, structure, and function [J]. J Chem Inf Model. 2021;61(10):4827–31.
21. Colovos C, Yeates TO. Verification of protein structures: patterns of nonbonded atomic interactions [J]. Protein Sci. 1993;2(9):1511–9.
22. Goldenberg O, Erez E, Nimrod G, Ben-Tal N. The ConSurf-DB: pre-calculated evolutionary conservation profiles of protein structures [J]. Nucleic Acids Res. 2009;37(Database issue):D323–7.
23. Craig DB, Dombkowski AA. Disulfide by Design 2.0: a web-based tool for disulfide engineering in proteins [J]. BMC Bioinformatics. 2013;14:346.
24. De Brevern AG, Bornot A, Craveur P et al. PredyFlexy: flexibility and local structure prediction from sequence [J]. Nucleic Acids Res. 2012;40(Web Server issue):W317–22.
25. Ozvoldik K, Stockner T, Rammner B, Krieger E. Assembly of biomolecular gigastructures and visualization with the vulkan graphics API [J]. J Chem Inf Model. 2021;61(10):5293–303.
26. Krieger E, Vriend G. YASARA View - molecular graphics for all devices - from smartphones to workstations. [J] Bioinf. 2014;30(20):2981–2.
27. Maier JA, Martinez C, Kasavajhala K, et al. ff14SB: improving the accuracy of protein side chain and backbone parameters from ff99SB [J]. J Chem Theory Comput. 2015;11(8):3696–713.
28. Wang H, Gao X, Fang J. Multiple staggered mesh Ewald: boosting the accuracy of the smooth particle mesh Ewald method [J]. J Chem Theory Comput. 2016;12(11):5596–608.
29. Qi H, Wang T, Li H, et al. Sequence- and Structure-Based mining of thermostable D-Allulose 3-Epimerase and Computer-Guided protein engineering to improve enzyme activity [J]. J Agric Food Chem. 2023;71(47):18431–42.
30. Chen L, Yu K, Ma A, et al. Enhanced thermostability of nattokinase by Computation-Based rational redesign of flexible regions [J]. J Agric Food Chem. 2024;72(25):14241–54.
31. Wedemeyer WJ, Welker E, Narayan M, Scheraga HA. Disulfide Bonds Protein Fold [J] Biochem. 2000;39(15):4207–16.
32. Lu M, Xu J, Wang Z, et al. In Silico mining and identification of a novel lipase from Paenibacillus larvae: rational protein design for improving catalytic performance [J]. Enzyme Microb Technol. 2024;179:110472.
33. Sun Z, Liu Q, Qu G, et al. Utility of B-Factors in protein science: interpreting rigidity, flexibility, and internal motion and engineering thermostability. [J] Chem Rev. 2019;119(3):1626–65.
34. Makepeace KAT, Serpa JJ, Petrotchenko EV, Borchers CH. Comprehensive identification of disulfide bonds using non-specific proteinase K digestion and CID-cleavable crosslinking analysis methodology for orbitrap LC/ESI-MS/MS data [J]. Methods. 2015;89:74–8.
35. Li Y, Tang X, Chen L, et al. Improvement of the fibrinolytic activity, acid resistance and thermostability of nattokinase by surface charge engineering [J]. Int J Biol Macromol. 2023;253:127373.
36. Cai D, Zhu C, Chen S. Microbial production of Nattokinase: current progress, challenge and prospect [J]. World J Microbiol Biotechnol. 2017;33(5):84.
37. Zhao L, Ma Z, Zhang L et al. Synthesis of value-added uridine 5′-diphosphate-glucose from sucrose applying an engineered sucrose synthase counteracts the activity-stability trade-off [J]. Food Chem, 2025, 464(Pt 2):141765.
38. Yang Z, Zeng X, Zhao Y, Chen R. AlphaFold2 and its applications in the fields of biology and medicine [J]. Signal Transduct Target Ther. 2023;8(1):115.
39. Yu H, Dalby PA. A beginner's guide to molecular dynamics simulations and the identification of cross-correlation networks for enzyme engineering [J]. Methods Enzymol. 2020;643:15–49.
40. Jiang S, Zhang Z, Gu Q, et al. Rational design to enhance the catalytic activity of acetylcholinesterase and mitigate Trichlorfon toxicity in vitro [J]. Int J Biol Macromol. 2024;283(Pt 4):138001.
41. Panja AS, Maiti S, Bandyopadhyay B. Protein stability governed by its structural plasticity is inferred by physicochemical factors and salt bridges [J]. Sci Rep. 2020;10(1):1822.
42. Xiang Z, Zhang X-C, Shi H-L, et al. Enhancing the thermostability of the leucine dehydrogenase from Planifilum fimeticola through rational design of the flexible region [J]. Mol Catal. 2024;559:114048.
43. Lai R, Li G, Cui Q. Flexibility of Binding Site is Essential to the Ca^{2+} Selectivity in EF-Hand Calcium-Binding Proteins [J]. J Am Chem Soc. 2024;146(11):7628–39.
44. Liu Z, Zhao H, Han L, et al. Improvement of the acid resistance, catalytic efficiency, and thermostability of nattokinase by multisite-directed mutagenesis [J]. Biotechnol Bioeng. 2019;116(8):1833–43.
45. Guo Q, Zheng LJ, Luo X, et al. Engineering Escherichia coli for d-Allulose production from d-Fructose by fermentation [J]. J Agric Food Chem. 2021;69(45):13578–85.
46. Lobstein J, Emrich CA, Jeans C, et al. SHuffle, a novel Escherichia coli protein expression strain capable of correctly folding disulfide bonded proteins in its cytoplasm [J]. Microb Cell Fact. 2012;11:56.
47. Ni H, Guo PC, Jiang WL, et al. Expression of nattokinase in Escherichia coli and renaturation of its inclusion body [J]. J Biotechnol. 2016;231:65–71.
48. Chen JP, Gong JS, su C, et al. Improving the soluble expression of difficult-to-express proteins in prokaryotic expression system via protein engineering and synthetic biology strategies [J]. Metab Eng. 2023;78:99–114.
49. García-Arrazola R, Siu SC, Chan G et al. Evaluation of a pH-stat feeding strategy on the production and recovery of Fab′ fragments from E. coli [J]. Biochemical Engineering Journal, 2005, 23(3): 221–30.

Publisher's note